Supporting Information

Anionic shell shields a cationic core allowing for uptake and release of polyelectrolytes within core-shell responsive microgels

Arjan P. H. Gelissen,[a,§] Andrea Scotti,[a,§] Sarah K. Turnhoff,[a,§] Corinna Janssen,[a] Aurel Radulescu,[b] Andrij Pich,[c] Andrey A. Rudov, [d,e] Igor I. Potemkin[d,e,f] and Walter Richtering[a]

[a]Institute of Physical Chemistry, RWTH Aachen University, 52056 Aachen, Germany, European Union

[b]Jülich Centre for Neutron Science, Outstation at MLZ, 85747 Garching, Germany

[c]Institute of Technical and Macromolecular Chemistry, RWTH Aachen University, 52056 Aachen, Germany

[d]Physics Department, Lomonosov Moscow State University, Moscow 119991, Russian Federation

[e] DWI – Leibniz-Institute for Interactive Materials, Forckenbeckstr. 50, 52074 Aachen, Germany

[f] National Research South Ural State University, Chelyabinsk 454080, Russian Federation

[§]These authors contributed equally to this work.

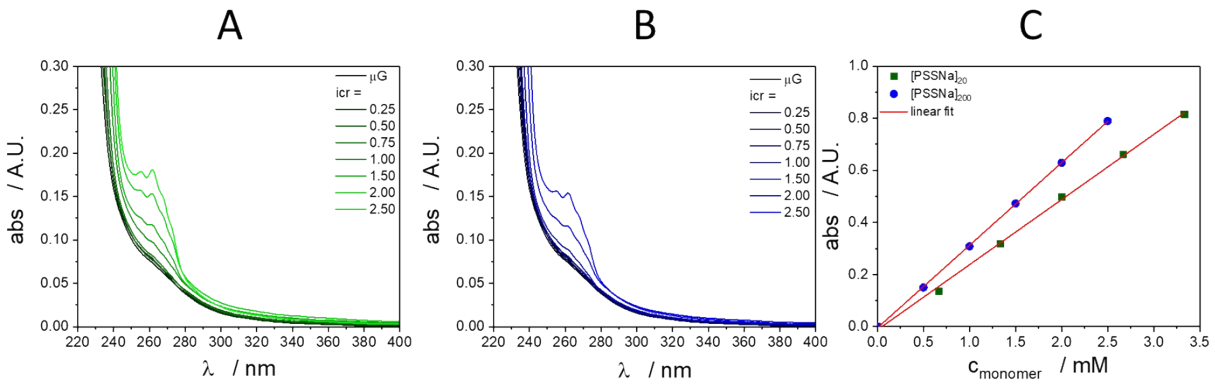

Figure S1: A) Absorption spectra of supernatant containing $[PSSNa]_{20}$ after mixing with a core-shell microgel at different charge ratios and subsequent centrifugation step. B) Absorption spectra of supernatant containing $[PSSNa]_{200}$ after mixing with a core-shell microgel at different charge ratios and subsequent centrifugation step. C) Calibration curves of $[PSSNa]_x$ with x = 20 (green squares) or 200 (blue circles).

Table S1: Calibration Absorbance and Concentration of $[PSSNa]_x$ in a Hellma 100 QS cuvette (10 mm).

	λ = 262 nm
$[PSSNa]_{20}$	E = 0.25 · c
$[PSSNa]_{200}$	E = 0.31 · c

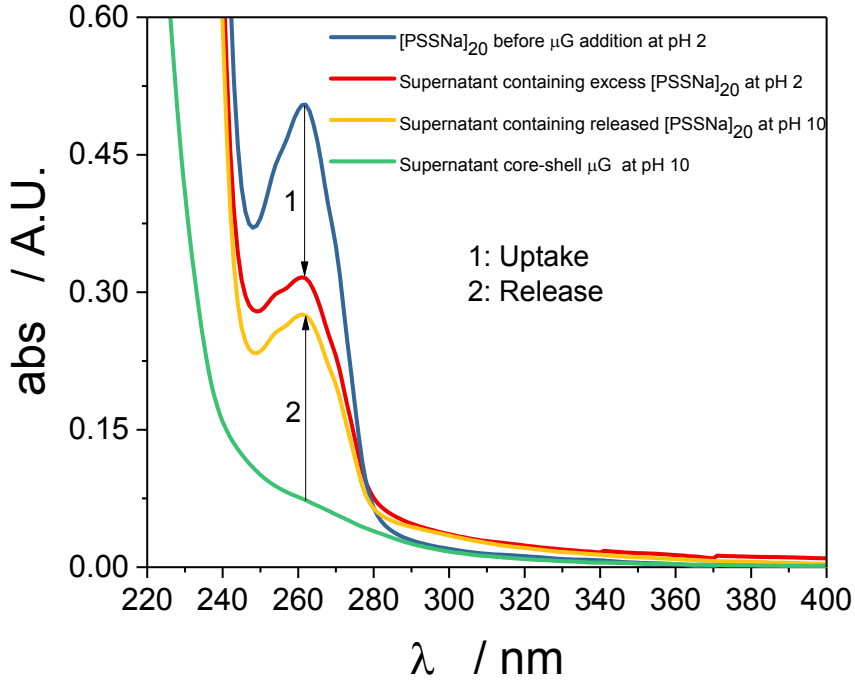

Figure S2: UV-Vis spectra of $[PSSNa]_{20}$ measured with the buffer solution as a reference. The blue line depicts the spectrum of the sample without microgel at pH 2. The red line depicts the spectrum of the

supernatant after centrifugation of the MPEC at pH 2. The green line depicts the supernatant after a pH-jump to basic pH. The absorbance at $\lambda = 262$ nm was used to calculate the concentration of $[PSSNa]_{20}$ using a calibration curve and applying Lambert-Beer.

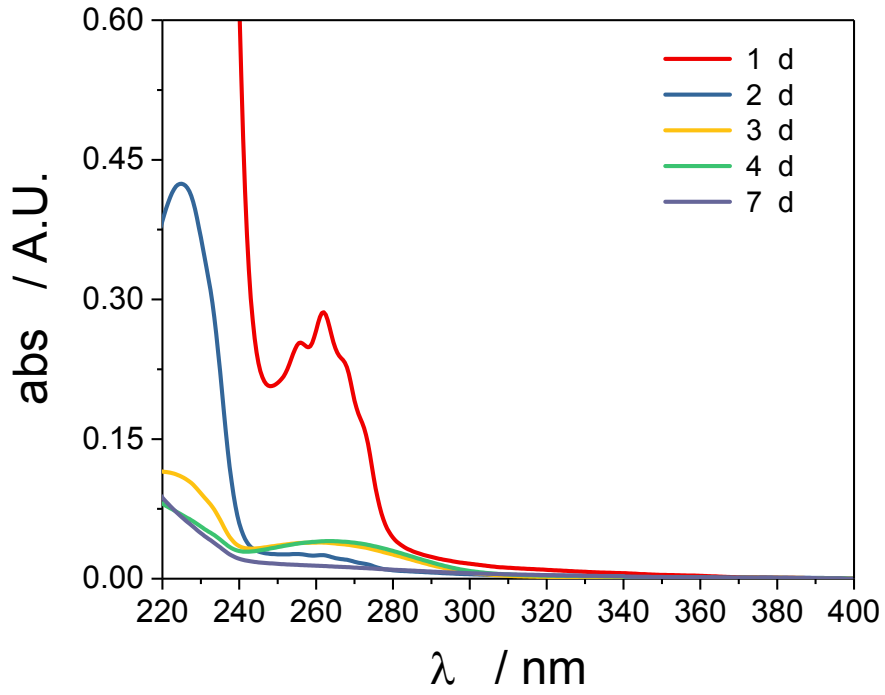

Figure S3: UV-Vis spectra of $[PSSNa]_{20}$ measured after a pH jump from 2 to 10 from the core-shell µG. The chromophore [PSSNa]20 could be detected in the supernatant after centrifugation.

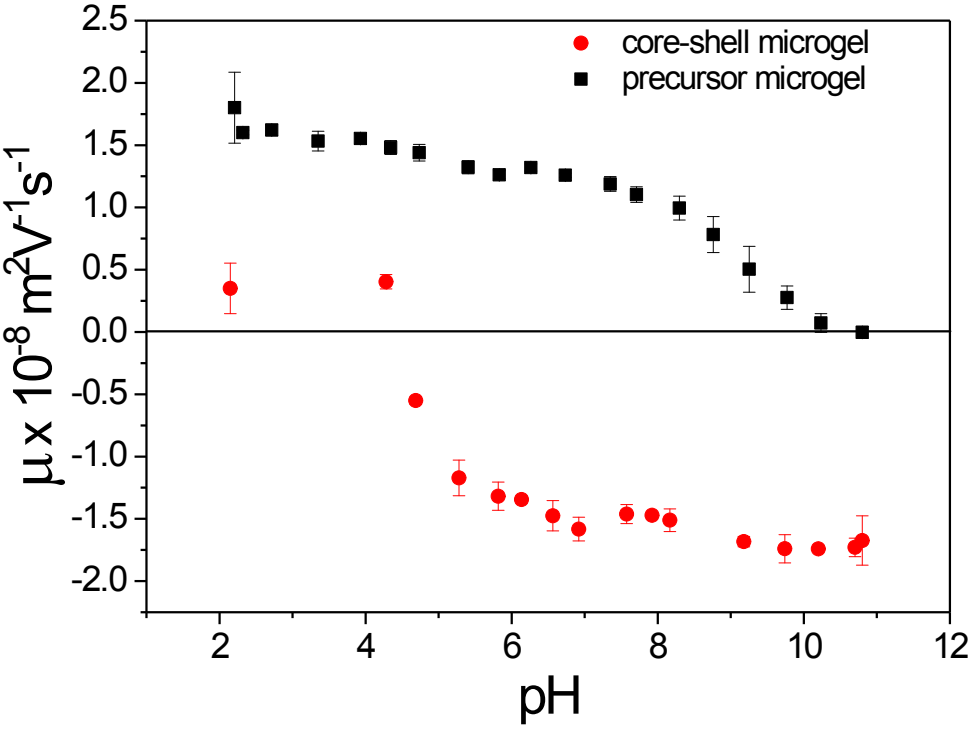

Figure S4: Dependence of the electrophoretic mobility of the precursor microgel and core-shell microgel on the pH. The electrophoretic mobility was determined in bidistilled water. Titration process was performed from pH 11 to pH 3 using 0.1 M NaOH and 0.1 M HCl. Measurements were performed at 20 °C.

Potentiometric Titration

To analyze the chargeable moieties in the microgel, 75 mg of the microgel were dissolved in 40 ml of water and transferred to a titration cell. The pH was adjusted to 11 with 0.1 M NaOH for the [NIPAM-co-APMH] – [NIPAM-co-MIA]. The pH was adjusted to 2.5 with 0.1 M HCl for the NIPAM-co-APMH. After the solution was allowed to equilibrate for 15 min, portions of 2 µL of 0.1 M HCl or NaOH respectively, were added by a Methrohm 665 autotitrator. Conductivity and pH were measured. The titrations were performed at 20°C.

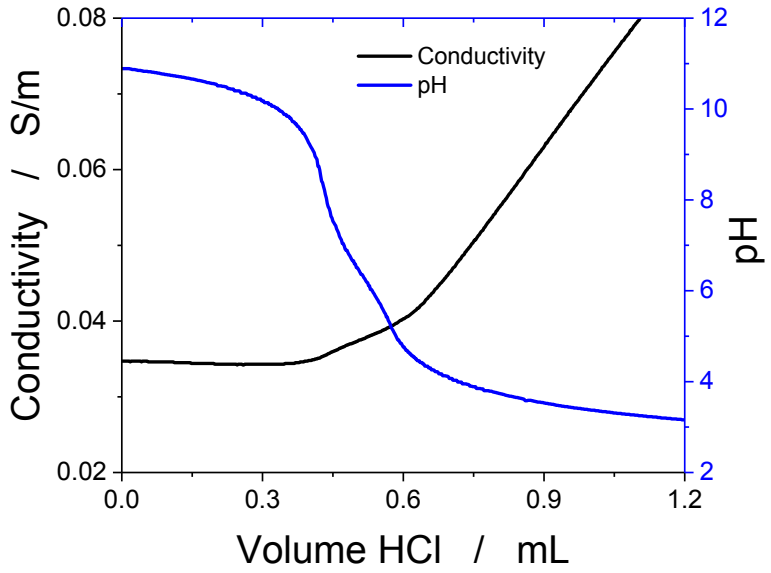

Figure S5a: Potentiometric titration of the [NIPAM-co-APMH]-[NIPAM-co-MIA] microgel. Conductivity and pH are measured by titrating with 0.1 M HCl.

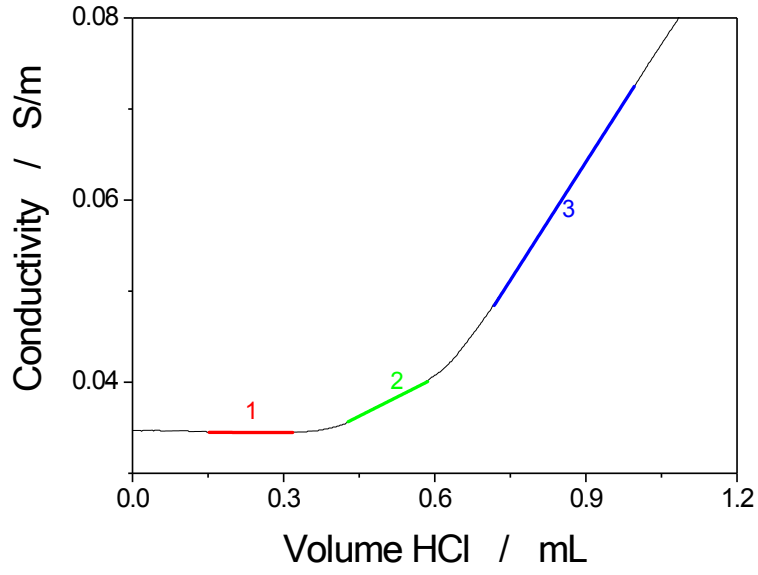

Figure S5b: Linear regression of different domains of the conductivity curve of the [NIPAM-co-APMH]-[NIPAM-co-MIA] microgel.

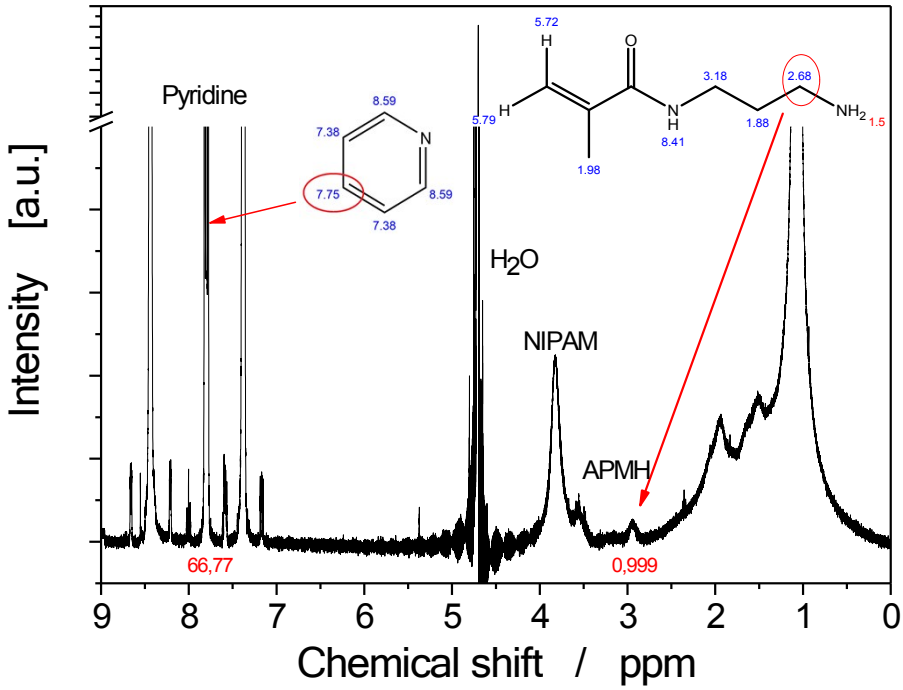

Figure S6: [1]H-NMR of the [NIPAM-co-APMH]-[NIPAM-co-MIA] microgel.

Figure S3 shows the [1]H-NMR spectrum of the [NIPAM-co-APMH]-[NIPAM-co-MIA] microgel with pyridine as an internal standard. The amount of APMH corresponds to 0.142 mmol/g. The amount of MIA corresponds to 0.355 mmol/g.

For most applications, MPEC-formation is considered successful when only single microgels interact with multiple polyelectrolyte chains. The opposite scenario, a single polyelectrolyte-chain interacting with multiple microgels is undesired. To achieve successful MPEC-formation, the timescales of adsorption and coagulation are crucial. Assuming the adsorption process being irreversible and diffusion controlled, the rate of polyelectrolyte adsorption is given by:[41]

$$k_{ads} = 4\pi \cdot R_{h,\mu G} \cdot D_{PE} \cdot c_{PE} \qquad (1)$$

with $R_{h,\mu G}$ corresponding to the hydrodynamic radius of the microgel, D_{PE} to the polyelectrolyte diffusion coefficient and c_{PE} to the polyelectrolyte concentration. The competing process is the collision of two microgels, since microgels partly covered with polyelectrolyte can strongly interact and coagulate. In a first approximation, this process can be described by:[42]

$$k_{coll} = 4\pi \cdot R_{h,\mu G} \cdot 2D_{\mu G} \cdot c_{\mu G} \quad (2)$$

with $D_{\mu G}$ corresponding to the microgel diffusion coefficient and $c_{\mu G}$ to the microgel concentration. To avoid MPEC-aggregation, the polyelectrolyte adsorption rate k_{ads} has to be large compared to the microgel collision rate k_{coll}:

$$\frac{k_{ads}}{k_{coll}} \gg 1 \quad (3)$$

To fulfill this condition, the uptake of polyelectrolyte by a microgel is achieved by dropwise addition of a microgel dispersion into an excess solution of polyelectrolytes to keep $c_{\mu G}$ low. Another important aspect is the size (or diffusion coefficient) of the microgel compared to the size (or diffusion coefficient) of the polyelectrolyte chain. When both are in the same order of magnitude, bridging of microgels may occur. This phenomenon cannot be neglected when small microgels are used. Microgels are not rigid particles, but porous polymer networks. Therefore, the size of the polyelectrolyte-chain and the microgels mesh size are decisive parameter whether the polyelectrolyte-chain may or may not penetrate the polymer network.

Pulsed field gradient NMR and PSS characterization

Pulsed field gradient NMR experiments were performed with a Bruker DSX 500 Spectrometer at 18°C, Δ = 20 ms and g_{max} = 1278 G/cm. $[PSSNa]_x$ of different chain lengths (x = 20, 200, 2000) were dissolved in a deuterated buffer solution with I = 50 mM.

NMR diffusion experiments using pulsed field gradients (PFG) and a stimulated echo sequence were performed to measure the diffusion coefficient D_{PE} of $[PSSNa]_x$ with different chain lengths. The results are listed in Table S2. The aromatic signal was used for evaluation. The resulting diffusion coefficient was converted into a R_h using Stokes-Einstein equation.

Table S2: Results for diffusion coefficient and hydrodynamic radius of $[PSSNa]_x$ with different chain lengths, determined via PFG at Δ = 20 ms and g_{max} = 1278 G/cm.

Polyelectrolyte-Chain	Signal [ppm downfield from TMS standard]	D_{PE} [$m^2 \cdot s^{-1}$]	R_h [nm]
$[PSSNa]_{20}$	8.082 – 5.137	$5.79 \cdot 10^{-11}$	3
$[PSSNa]_{200}$	8.242 – 5.495	$1.91 \cdot 10^{-11}$	10
$[PSSNa]_{2000}$	8.585 – 5.962	$2.03 \cdot 10^{-12}$	93

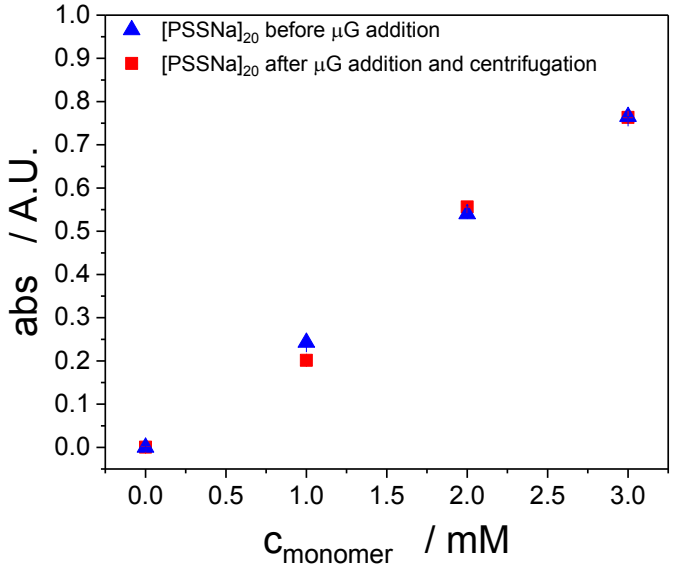

Figure S7: Absorbance of a $[PSSNa]_{20}$ solution before and after addition of a neutral microgel.

Figure S7 shows that a neutral microgel does not interact with the guest molecules. Microgel and polyelectrolyte were mixed in the same procedure as for the MPEC formation for the charged microgels. The supernatant of the mixture of polyelectrolyte and microgel exhibits the same absorbance as the pure polyelectrolyte solution demonstrating that the neutral microgel does not take up any polyelectrolyte.

Model to fit scattering data

We assume a constant polymer volume fraction starting from the microgel center, which decays gradually at the periphery to mimic the fuzziness of the microgels.[1, 2]

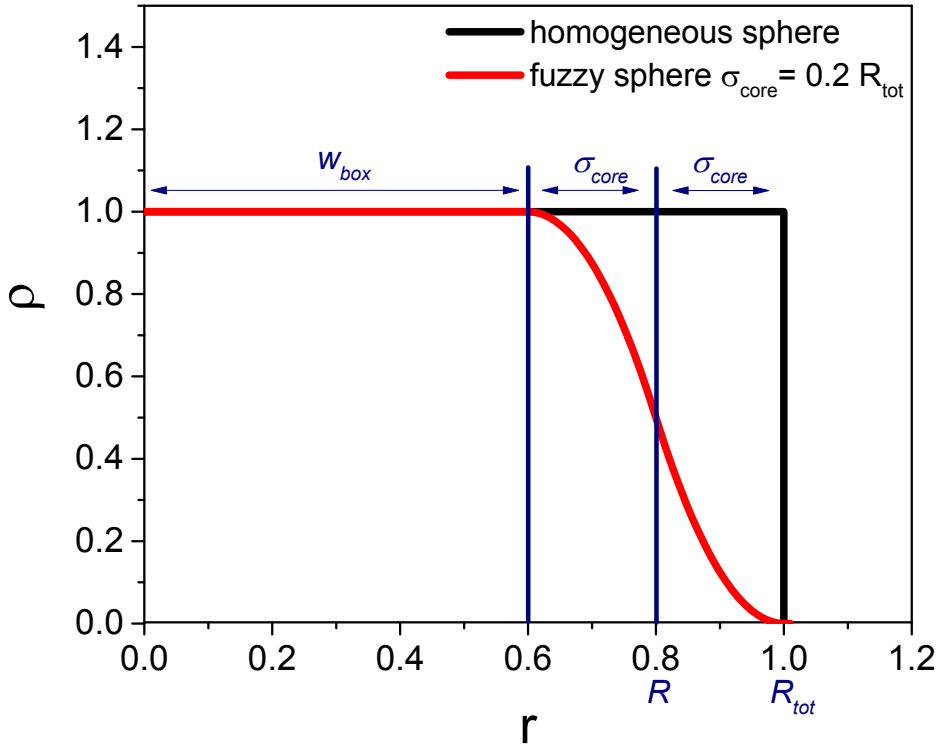

Figure S8: Schematic representation of a fuzzy sphere density profile.

The radial density profile ρ can also be expressed by the half-width radius R and σ using a parabolic shape. The volume V of the microgels is $4\pi \cdot V_n$.

$$V_n = \frac{R^3}{3} + \frac{R \cdot \sigma^2}{6} \tag{S 1}$$

$$\begin{aligned}
&\rho = 1 && if\ r \leq (R-\sigma)\\
&\rho = 1 - \frac{1}{2} \cdot \frac{[(R-r)+\sigma]^2}{\sigma^2} && if\ (R-\sigma) < r \leq R\\
&\rho = \frac{1}{2} \cdot \frac{[(R-r)+\sigma]^2}{\sigma^2} && if\ R < r \leq (R-\sigma)\\
&\rho = 0 && if\ (R+\sigma) < r
\end{aligned} \tag{S 2}$$

The benefit of this profile is the possibility to calculate the Fourier transformation analytically as shown in Equation S3:

$$\varphi = \frac{1}{V_n} \cdot \left(\left(\frac{r}{\sigma^2} + \frac{1}{\sigma}\right) \cdot \frac{\cos\left(q \cdot (r+\sigma)\right)}{q^4} + \left(\frac{r}{\sigma^2} - \frac{1}{\sigma}\right) \cdot \frac{\cos\left(q \cdot (r-\sigma)\right)}{q^4} - \frac{3\sin\left(q \cdot (r+\sigma)\right)}{q^5 \cdot \sigma^2} - \frac{3\sin\left(q \cdot (r-\sigma)\right)}{q^5 \cdot \sigma^2} - \frac{2 \cdot r\cos\left(q \cdot r\right)}{q^4 \cdot \sigma^2} + \frac{6\,sin(q \cdot r)}{q^5 \cdot \sigma^2} \right) \quad \text{(S 3)}$$

Weighting φ with the scattering contrast $\Delta\rho$ and microgel volume V gives the scattering amplitude A. An analytical expression for the scattering amplitude enables to model compartmentalized microgels with a core-shell, a core-shell-shell or even a multiple shell structure in an easy fashion by simply summarizing scattering amplitudes. Hollow microgels can be modeled using $\Delta\rho_{core} = 0$. In the following, a step by step demonstration of modeling the scattering amplitude of a core-shell-shell is described:

$$A_{core}(q, R_{core}, \sigma_1, \Delta\rho_{core}) = \Delta\rho_{core} \cdot V_{core} \cdot \varphi_{core}(q, R_{core}, \sigma_1) \quad \text{(S 4)}$$

$$A_{sh,1}(q, R_{sh,1}, \sigma_2, \Delta\rho_{sh,1}, R_{core}, \sigma_1) = \Delta\rho_{sh,1} \cdot \left[V_{sh,1} \cdot \varphi(q, R_{sh,1}, \sigma_2,) - V_{core} \cdot \varphi(q, R_{core}, \sigma_1)\right]$$

$$A_q = A_{core}(q, R_{core}, \sigma_1, \Delta\rho_{core}) + A_{sh,1}(q, R_{sh,1}, \sigma_2, \Delta\rho_{sh,1}, R_{core}, \sigma_1)$$

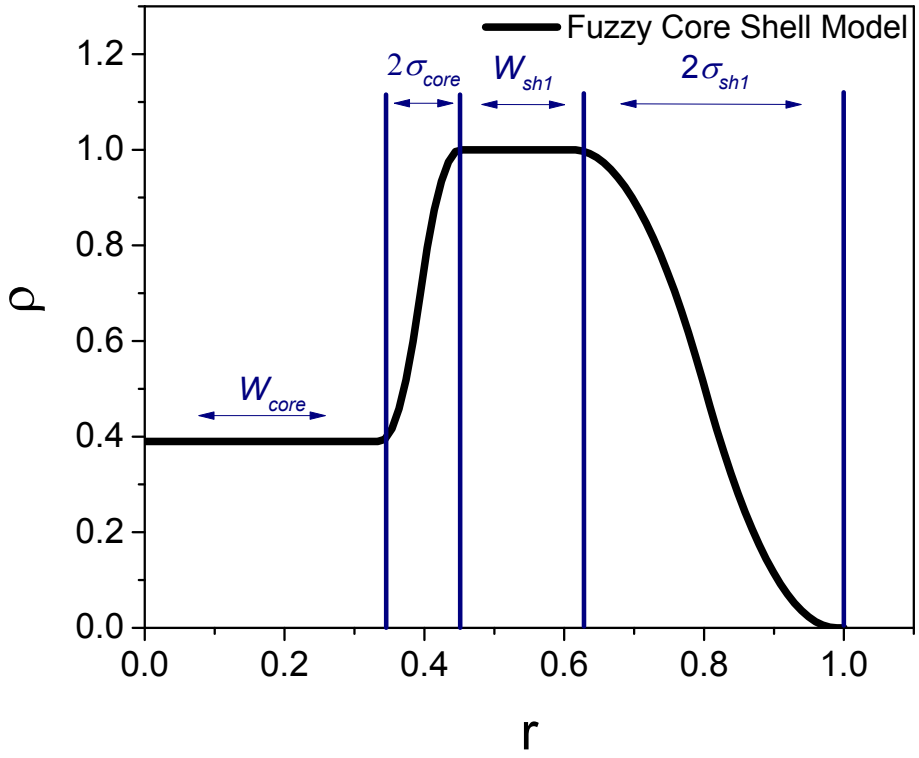

Figure S9: Schematic representation of core-shell density profile.

The modeled expression for the scattering intensity has to be extended with a Lorentzian function to account for the scattering contribution of internal fluctuations within the microgel network. This function is simply added to the squared scattering amplitude $A^2(q)$ and contributes significantly to $I(q)$ at 'high' q-values. The correlation length ξ of the fluctuations corresponds to the mesh-size of the microgel and $I_L(0)$ denotes the intensity at $q = 0$.

$$I_L(q) = \frac{I_L(0)}{[1 + q^2\xi^2]} \qquad \text{(S 5)}$$

Besides internal fluctuation within the network, also incoherent scattering contributes to the measured intensity. Incoherent scattering does not contribute to the interference pattern, so only a constant background value I_{back} is added to $A^2(q)$. Besides poorer statistics due to the geometry of the detector, the presence of incoherent scattering affects especially in a neutron scattering experiment the accuracy of the 'high' q-values.

Microgels are synthetic polymeric networks. So far, the assumption was made that all microgels are exactly identical in size (monodisperse), which is synthetically extremely difficult to achieve. The scattering curve of polydisperse microgels is an average over all N form factors $P_i(q)$ weighted with the respective scattering contrast $\Delta\rho_i$ and volume V_i of the corresponding i-th microgel.

$$\Delta I(q) = I(0) \cdot \sum_{i=1}^{N} \Delta\rho_i^2 \cdot V_i^2 \cdot P_i(q) \tag{S 6}$$

Since the size distribution function of a microgel sample is not defined, the choice of certain distribution function is arbitrary. In this work a Gaussian distribution function was assumed with σ_{poly} as the relative microgel size polydispersity to fit the experimental data.

$$D\left(R,\langle R\rangle,\sigma_{poly}\right) = \frac{1}{\sqrt{2\pi \cdot \sigma_{poly}^2 \cdot \langle R\rangle^2}} exp\left[-\frac{(R-\langle R\rangle)^2}{2\sigma_{poly}^2 \cdot \langle R\rangle^2}\right] \tag{S 7}$$

In case of a SANS experiment, a wavelength distribution with a width σ_{smear} has to be taken into account as well as contributions from collimation and detector resolution.

$$R(\langle q\rangle,q) = \frac{q}{\sigma_{smear}^2} exp\left[-\frac{1}{2}\left(q^2 + \frac{\langle q\rangle^2}{\sigma_{smear}^2}\right)\right] I_0 \frac{\langle q\rangle q}{\sigma_{smear}^2} \tag{S 8}$$

Finally, all contributions are incorporated into the model and the experimental data can be fitted.

$$I^{mod}(\langle q\rangle) = n \int_0^\infty \int_0^\infty R(\langle q\rangle,q) D(R,\langle R\rangle,\sigma_{poly}) \left[A^2(q) + I_L(q) + I_{back}\right] dR dq \tag{S 9}$$

with:

$$n = c\left[\int_0^\infty \left[\varphi_{core}\rho_{core}V_{core} + \varphi_{sh,1}\rho_{sh,1}V_{sh,1} + \varphi_{sh,2}\rho_{sh,2}V_{sh,2}\right] D\left(R,\langle R\rangle,\sigma_{poly}\right) dR\right]^{-1}$$

Computer Simulations

A movie is provided in the Supporting Information, which shows that the microgel shell immediately expands and polyanions are released after a pH switch from 2 to 10. The linear chains have a length of N = 10 and a fraction of anionic groups of φ = 0.5. The used microgel C1S7 has the same characteristics (core size, fractions of charged groups) as in the article but comprises a bigger shell.

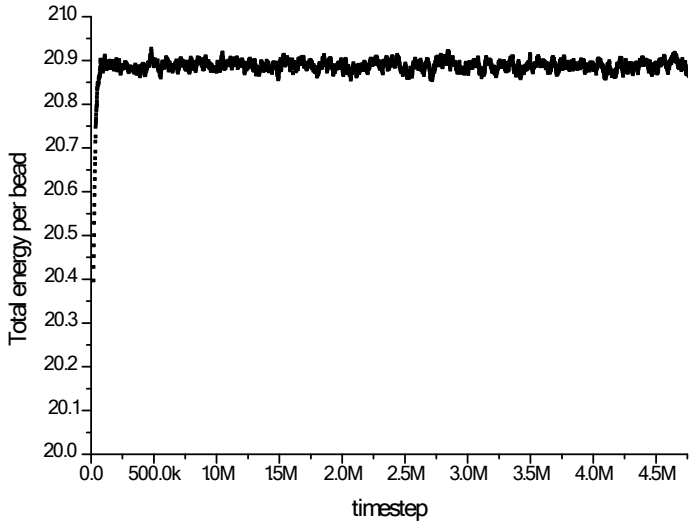

Fig. S10: Total energy per bead during uptake process as a function of time steps at N = 8 and φ = 0.25.

Supporting Literature

1. M. Stieger, W. Richtering, J. S. Pedersen and P. Lindner, J. Chem. Phys., 2004, **120**, 6197-6206.
2. I. Berndt, J. S. Pedersen and W. Richtering, Angew. Chem., Int. Ed., 2006, **45**, 1737-1741.